



R2E PROJECT
CERN – Building 157
CH-1211 Geneva 23
Switzerland

CERN Div./Group

EN/STI

EDMS Document No.

0000000

CHARM Radiation Test Report

RF Amplifier using VRF151G and BLF 574 Power RF Mosfets

DOCUMENT PREPARED BY:

Chihiro Omori
Mauro Paoluzzi

DOCUMENT CHECKED BY:

[Name]

This document describes the results of the radiation test of two power RF amplifiers.

1. User's Information

Concerned equipment	RF Power Amplifier
User	M.Paoluzzi/C.Ohmori
Device Under Test (DUT)	VRF151 and BLF574
Irradiation session 1	from 11/10/2017 to 16/10/2017
Irradiation session 2	from 18/10/2017 to 23/10/2017
Irradiation session 3	from 24/10/2017 to 3/10/2017
CHARM configuration	"Cu000"
Test position	R13

Specifications by	M.Paoluzzi/C.Ohmori
Tested by	M.Paoluzzi/C.Ohmori
HW development by	C.Ohmori
SW development by	C.Ohmori

2. Overview

Two identical setups, each bearing one RF Mosfet type (VRF151 and BLF574) have been used. The equipment installed in the radiation zone consist of a RF Power amplifier, an RF load, cooling fans and a radiation compensation reference device. The reference device is the same as used for the RF Power amplifier. The irradiated setups, installed in the equipment room, provide adequate RF driving for constant amplitude operation (100W) and frequency sweep from 0.5 MHz to 5 MHz. Compensation for the TID effects on the threshold voltage displacement is derived from the reference device response and applied to the RF Power Amplifier device.

The study aimed at evaluating the compensation effectiveness and the degradation of the amplifier characteristics in terms of maximum power, gain and phase variations.

During the session, the configuration of CHARM was copper target no shielding hereafter defined as "Cu0000".

Outline

CHARM RADIATION TEST REPORT	1
RF AMPLIFIER USING VRF151G AND BLF 574 POWER RF MOSFETS	1
1. USER'S INFORMATION	2
2. OVERVIEW	2
3. OBJECTIVES OF THE CAMPAIGN	4
4. DUT IDENTIFICATION AND OPERATING CONDITIONS	4
5. DESCRIPTION	4
6. TEST PROCEDURE: SETUP AND DESCRIPTION	4
6.1 TEST SETUP.....	4
6.2 TEST METHODOLOGY	6
7. FACILITY CONFIGURATION	6
8. EXPERIMENTAL RESULTS	9
8.1 BLF574	9
8.2 VRF151	12
9. CONCLUSIONS	13

3. Objectives of the campaign

The study aimed at evaluating the sensitivity to SE as well as TID compensation effectiveness and the degradation of the amplifier characteristics in terms of maximum power, gain and phase variations.

4. DUT identification and operating conditions

DUT Information			
Name	Type	Manufacturer	Package
VRF151	RF Mosfet	Microsemi	Ceramic case
BLF574	RF Mosfet	NXP	Ceramic case

Table 1: DUT(s) information.

5. Description

When exposed to ionizing and non-ionizing particles, RF Power Mosfets are affected by various radiation effects. Previous testing using Coabalt-60 radiation sources showed that the main effect is the threshold voltage displacement for which a compensation strategy has been devised.

The objective of this work is to enlarge the characterization to a more complex radioactive environment, evaluating the sensitivity to SE as well as TID compensation effectiveness and the degradation of the amplifier characteristics in terms of maximum power, gain and phase variations.

6. Test procedure: Setup and Description

6.1 Test setup

Two identical setups, each bearing same RF Mosfet type (VRF151 and BLF574) have been used. The equipment installed in the radiation zone consist of a RF Power amplifier, an RF load, cooling fans and a radiation compensation reference device. The reference device is the same as used for the RF Power amplifier and implements a constant drain current generator. In the circuit, the drain current is stabilized to a constant value by altering the gate voltage as required. The same gate voltage is then used to bias the RF Amplifier device. The portion of the setups installed in the equipment room, provide compensation for the TID effects on the threshold voltage as well as adequate RF driving for constant amplitude operation (100W) and frequency sweep from 0.5MHz to 5MHz.

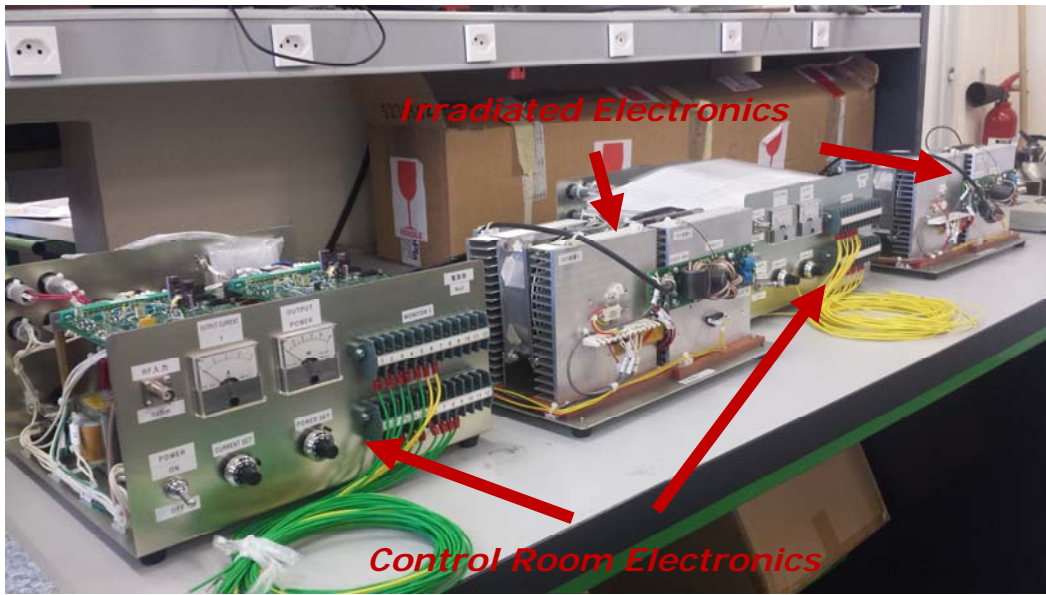


Figure 1: Boards and systems

The two setups are installed in Rack2 at 118 cm above ground. The system bearing the VRF151 devices is placed on the target side and BLF574 on the beam side (see §7 or details).

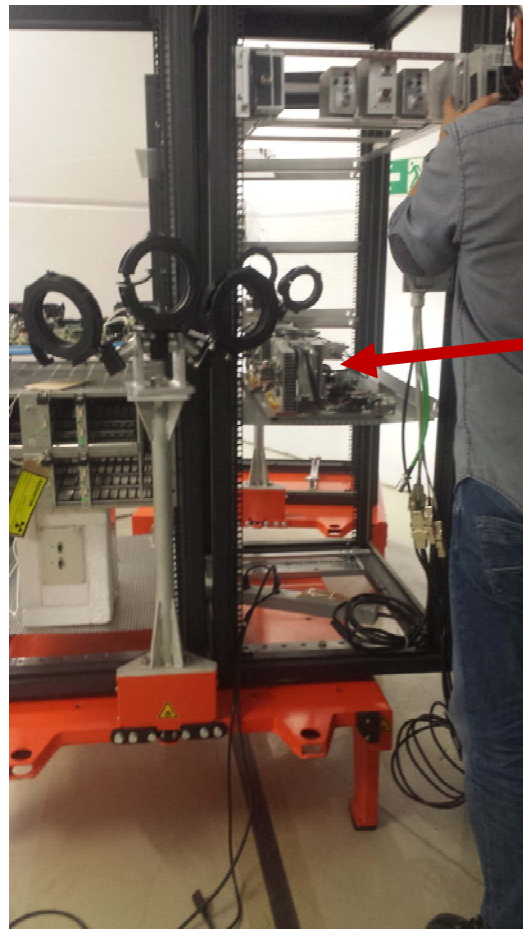


Figure 2: Setups on the rack at CHARM

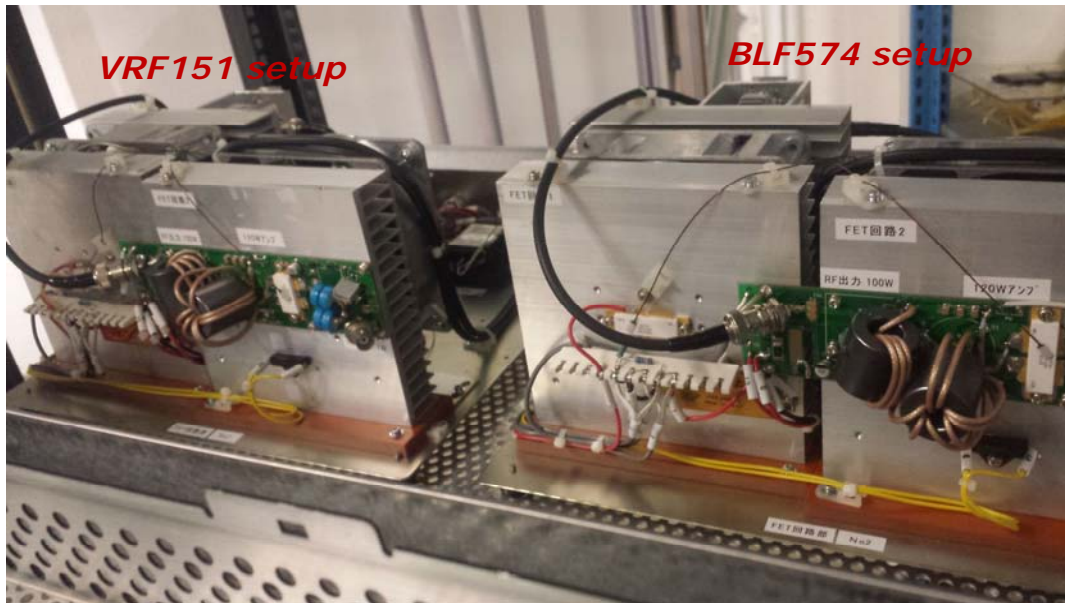


Figure 3: Detail of setups on the rack at CHARM

6.2 Test methodology

The two test setups are continuously operated during irradiation. Relevant signals related to threshold voltage compensation, rest currents, drive and output RF powers, operational frequency, amplifiers gain and phase shift are monitored.

7. Facility Configuration

The tests were carried out at the **C**ern **H**igh energy **A**ccelerator **M**ixed field facility (CHARM) of CERN. The details of the irradiation session can be found in the Charm User Dosimetry Document (UDD) [1]. The initial proton beam of 24 GeV for CHARM [2], [3], is extracted from the Proton Synchrotron (PS) accelerator. Then the beam is guided to the experimental area where it hit a cylindrical copper or aluminium target. The resulting secondary mixed radiation field is used to test electronic equipment at predefined test positions. Depending on the test position selected (from 1 to 13), the test equipment is exposed to different particle spectra. In addition, four movable blocks with a thickness of 40 cm and made out of concrete or iron can be placed between the target and the test locations.

The CHARM facility, because of the size of its experimental area can hosts different user experiments and the irradiation conditions are requested by the primary user, the other users withstand the conditions. During this run, we were a secondary user.

During the irradiation sessions the copper target was inside the irradiation area and all the shielding plates were open ('CuOOOO' configuration).

Configuration: Cu0000

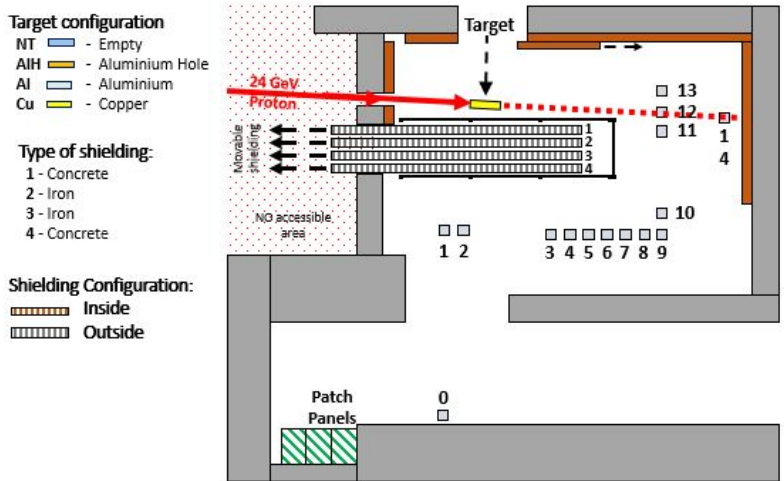


Figure 4: Facility Layout. The grey squares show the available test positions.

The Table 2 summarize the dose and the particles fluence of the irradiation session(s). The hardness factors $H_{50\%}$ and $H_{10\%}$ correspond to the HEH energy values for which the fluxes are 50% and 10% of the total HEH flux, respectively, while the POT is the number of protons impinging the target. The dose and the fluences are obtained by a detailed calibration performed by the CHARM team using the RadMon system [4]. In addition, in order to cross-check the calibration measurement of the dose and the fluences RadMon are placed close to the DUTs during the irradiation. A global uncertainty of 35% is estimated taking into account the error derived by both the Secondary Emission Chamber (SEC), which measure the POT and the CHARM dosimetry uncertainties.

	RUN 1		RUN 2		RUN 3	
Configuration	"Cu0000"		"Cu0000"		"Cu0000"	
Position	R13		R13		R13	
Target Inside	11-10-2017 15:48		18-10-2017 13:05		24-10-2017 17:44	
Target Outside	16-10-2017 21:59		23-10-2017 06:00		30-10-2017 14:26	
	Beam side	Target Side	Beam side	Target Side	Beam side	Target Side
	BLF574	VRF151	BLF574	VRF151	BLF574	VRF151
Dose [Gy]	640		561		736	
1MeV eq. fluence [cm²]	3.6 10 ¹²		3.2 10 ¹²		4.1 10 ¹²	
HEH fluence [cm²]	2.5 10 ¹²		2.2 10 ¹²		2.9 10 ¹²	
Total POT	1.48 10 ¹⁶		1.30 10 ¹⁶		1.70 10 ¹⁶	

Table 2: CHARM Configuration and run conditions

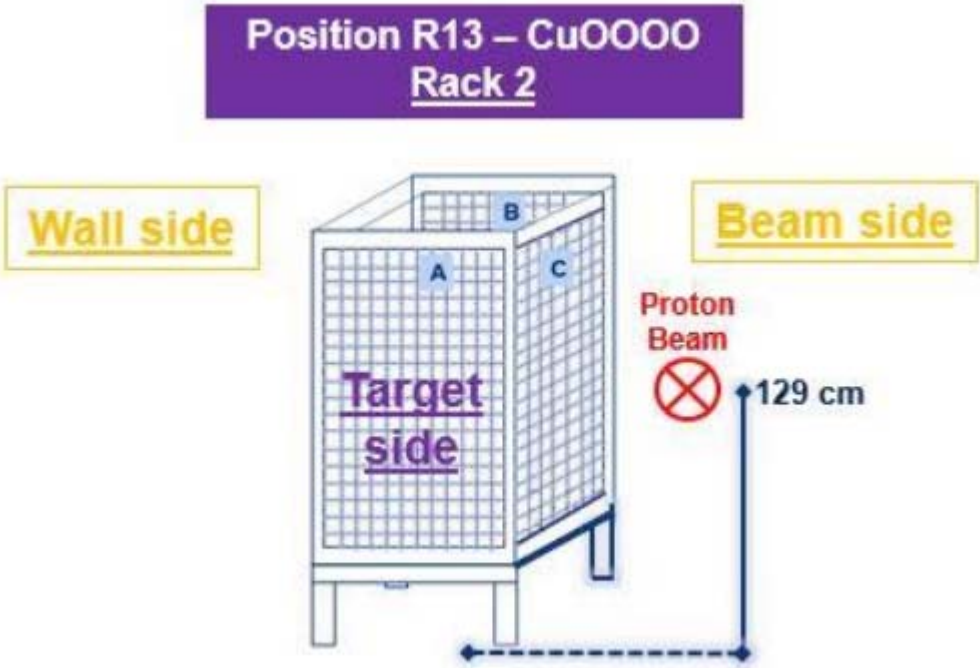


Figure 5: Rack 2 orientation in position 13.

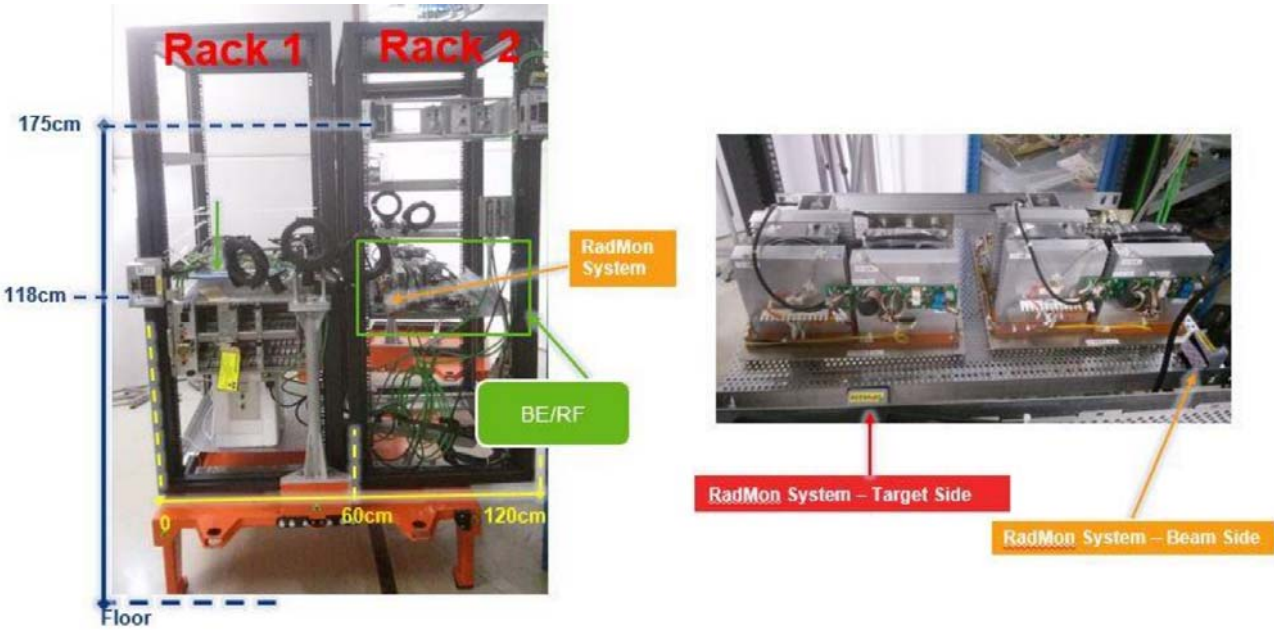


Figure 6: Racks 1 and Rack 2 assembly with RF Test Setup and RadMons in position 13.

8. Experimental results

The following figure plots the Dose, HEH fluence and 1MeV eq. neutrons fluence measured on the beam side. On the target side the values are $\approx 26\%$ lower.

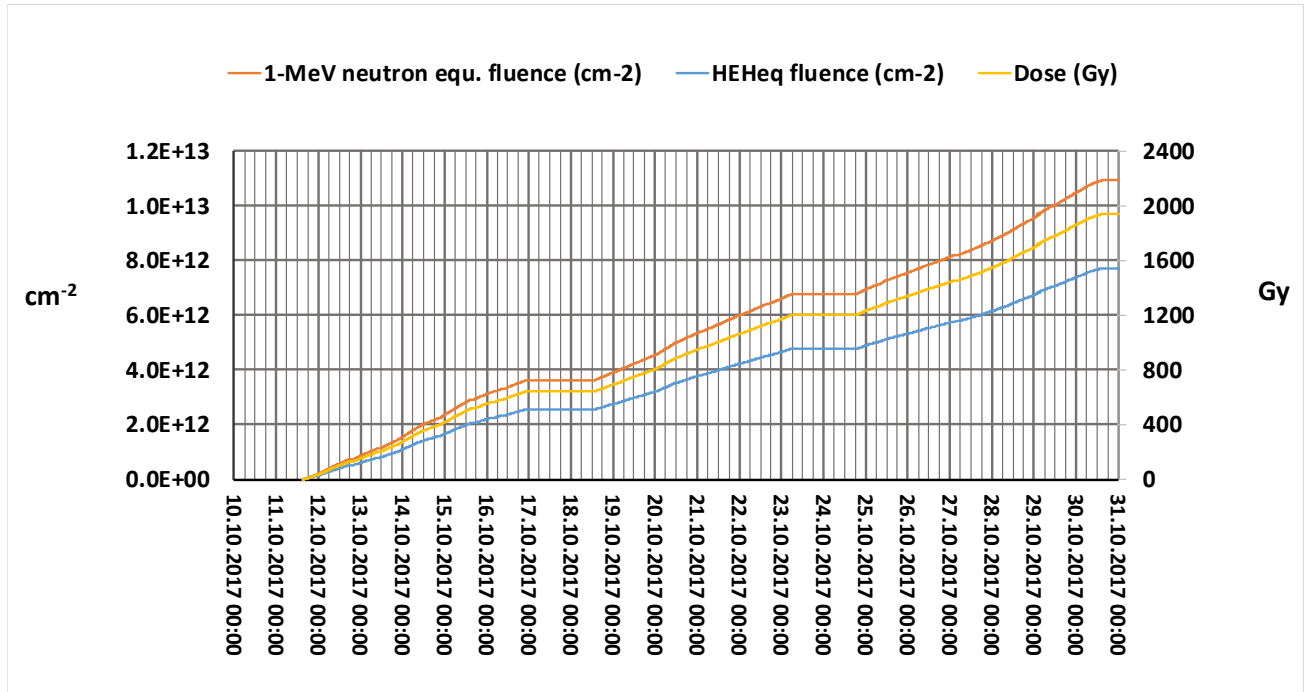


Figure 7: Beam Side Measured Dose, HEH fluence and 1MeV eq. neutrons fluence vs time .

8.1 BLF574

Shortly after starting the system, at a dose of few tens of Gy (but above 25 Gy), the circuitry compensating the radiation effects on the V_{TH} stopped working. Note that circuitry sits on the equipment room and is not submitted to radiation. The failure caused the RF amplifier to work in class C instead of class AB resulting in a substantial gain reduction. Figure 8 shows the response differences at 25Gy and 200Gy.

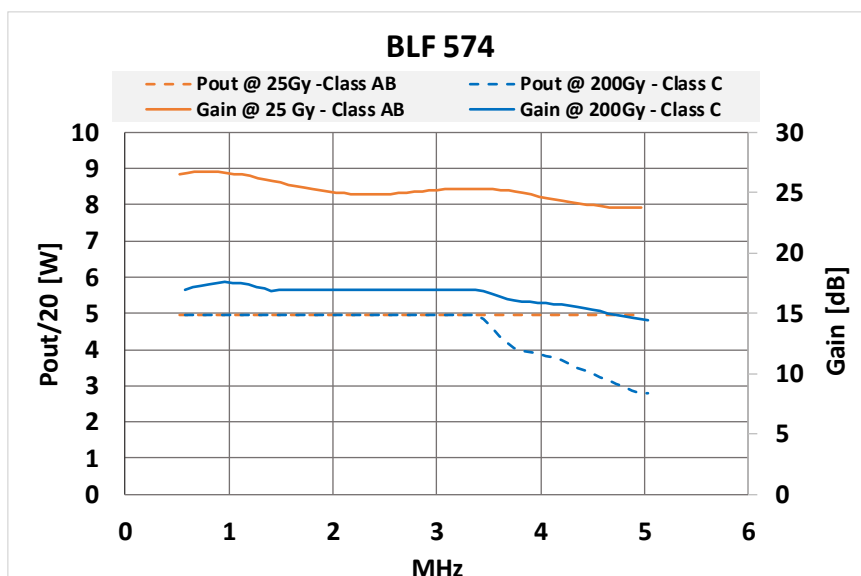


Figure 8: Gain and maximum Output Power Response vs Frequency at 25Gy and 200Gy .

During the technical stop between RUN 1 and RUN 2 the bias circuit was modified to manually control the gate bias voltage. The initial settings were such that a gate voltage around 1.5V was needed to achieve the nominal 1.5A rest current. At restart after modification, a substantial higher gate voltage was needed and a gate voltage adjusted around 2.5V only led to a rest current ≈ 0.8 A. This setting value was retained to limit the gate bias voltage and could be kept substantially unchanged during the whole run up to 1900Gy (see fig.9). One should note that V_{TH} reduction at increasing TID is expected from literature as well as previous testing using a Co-60 source in Takasaki, Japan (see fig.10). This behavior is thus unexpected.

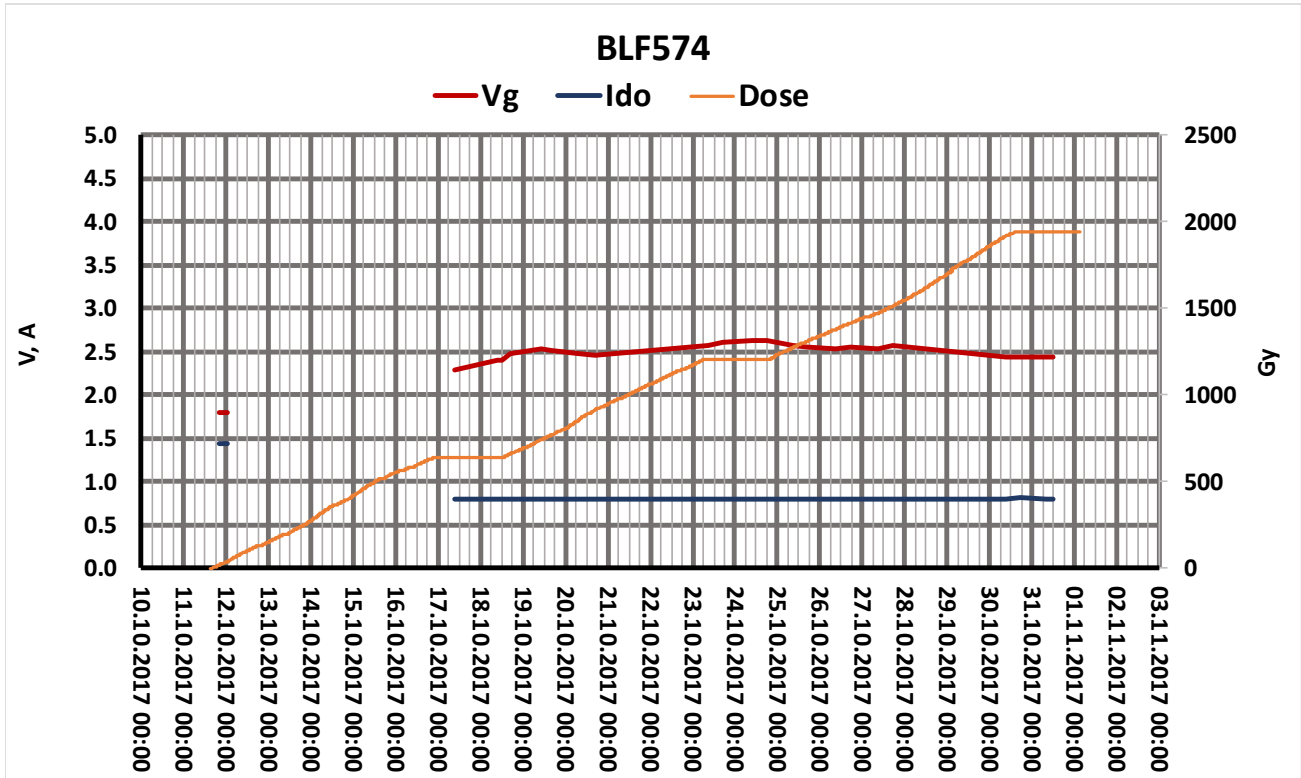


Figure 9: Gate Voltage, Rest current and Dose vs Time.

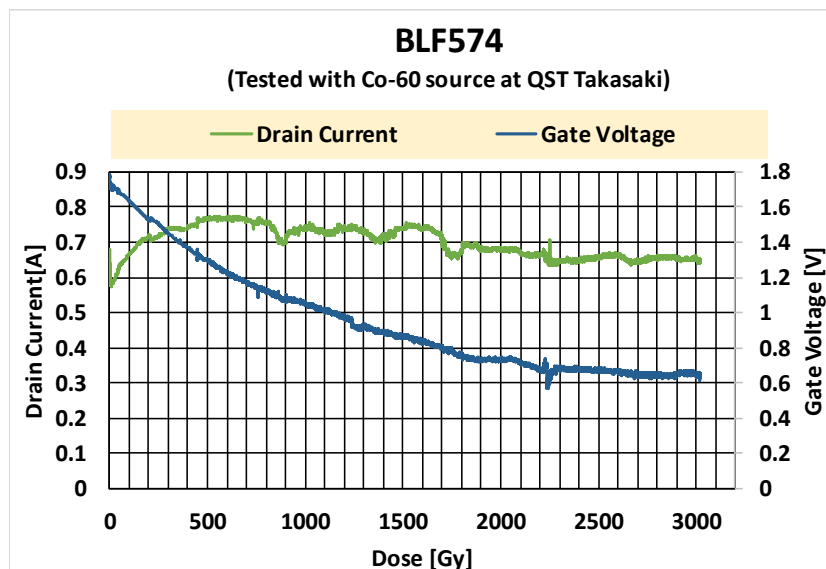


Figure 10: Measured Gate Voltage and Rest current vs Dose.

After restart, the gain showed an average decrease of about 8dB and the decrease continued as the dose increased (see fig.11). Despite the gain reduction, the RF driver stage had enough resources to drive the amplifier at the nominal 100W output power up to above a dose of 650Gy. Driver saturation effects only showed reaching the kGy level as shown by the green curve in fig.12. Despite the fact that above 1kGy the output power drastically dropped, the output signal, in terms of harmonic distortion, was substantially correct until the end of the test.

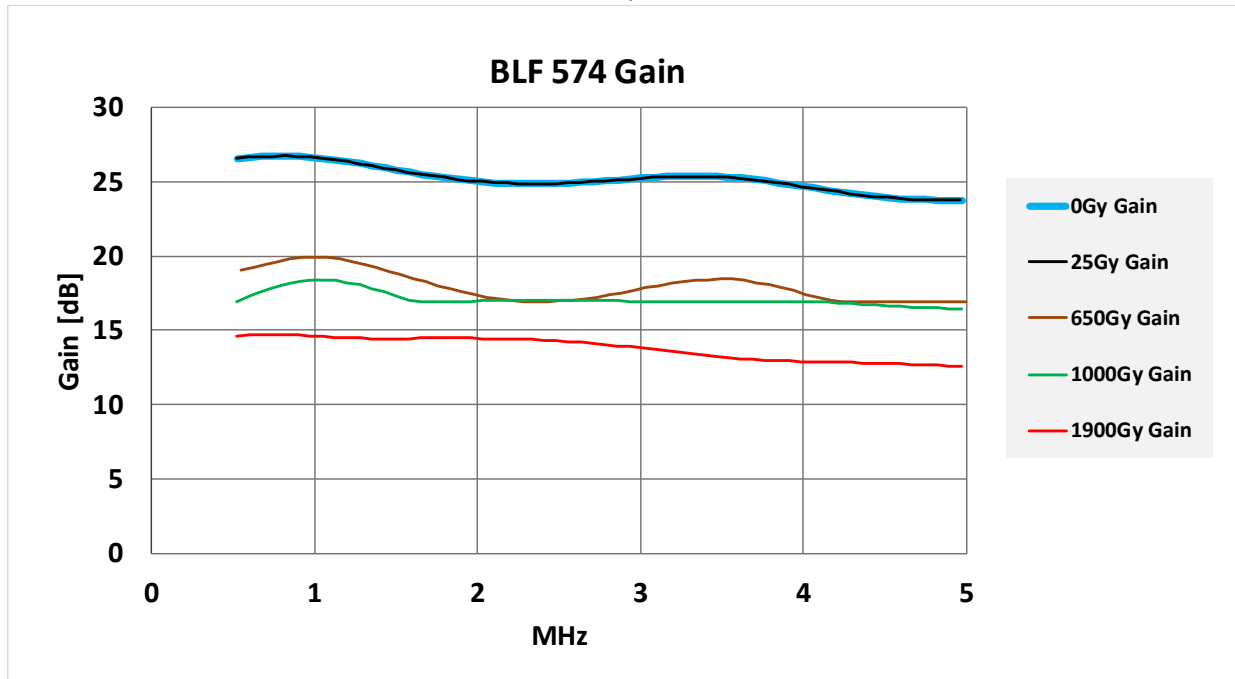


Figure 11: Gain response vs frequency at different TID.

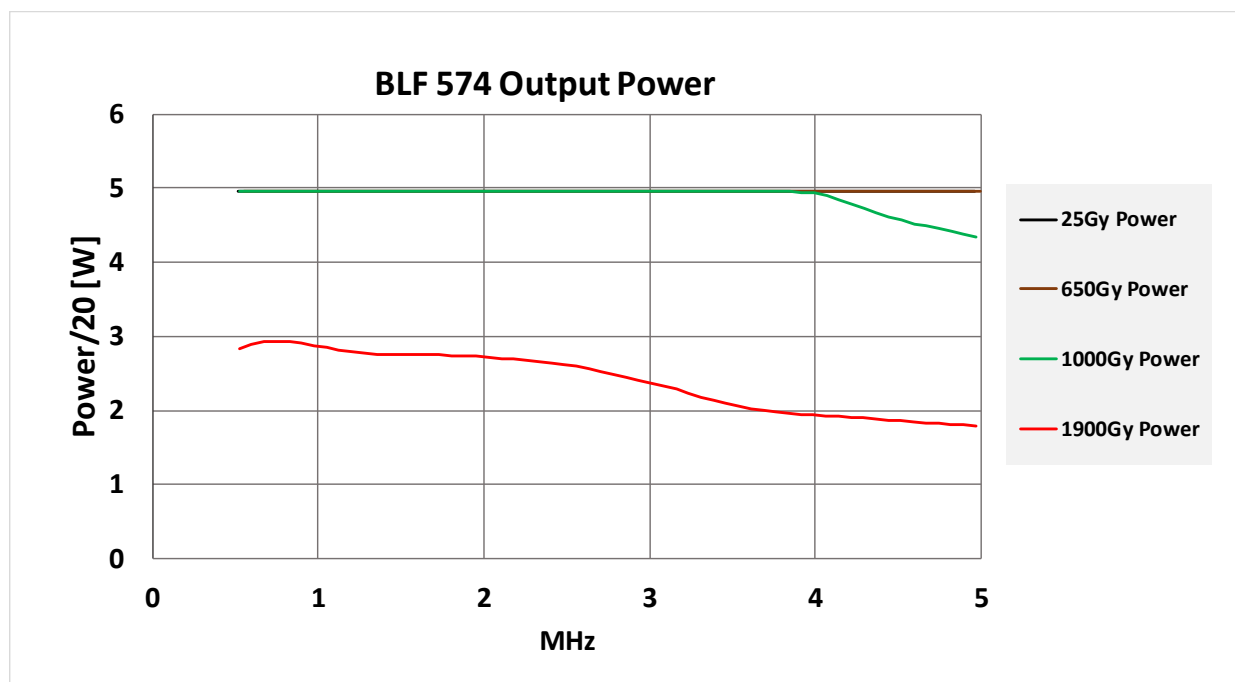


Figure 12: Output Power vs frequency at different TID.

8.2 VRF151

The VRF151 test showed a good correction of the TID effects on the V_{TH} shift. The drain current in the reference device stayed at the nominal value during the whole test. No SE occurred.

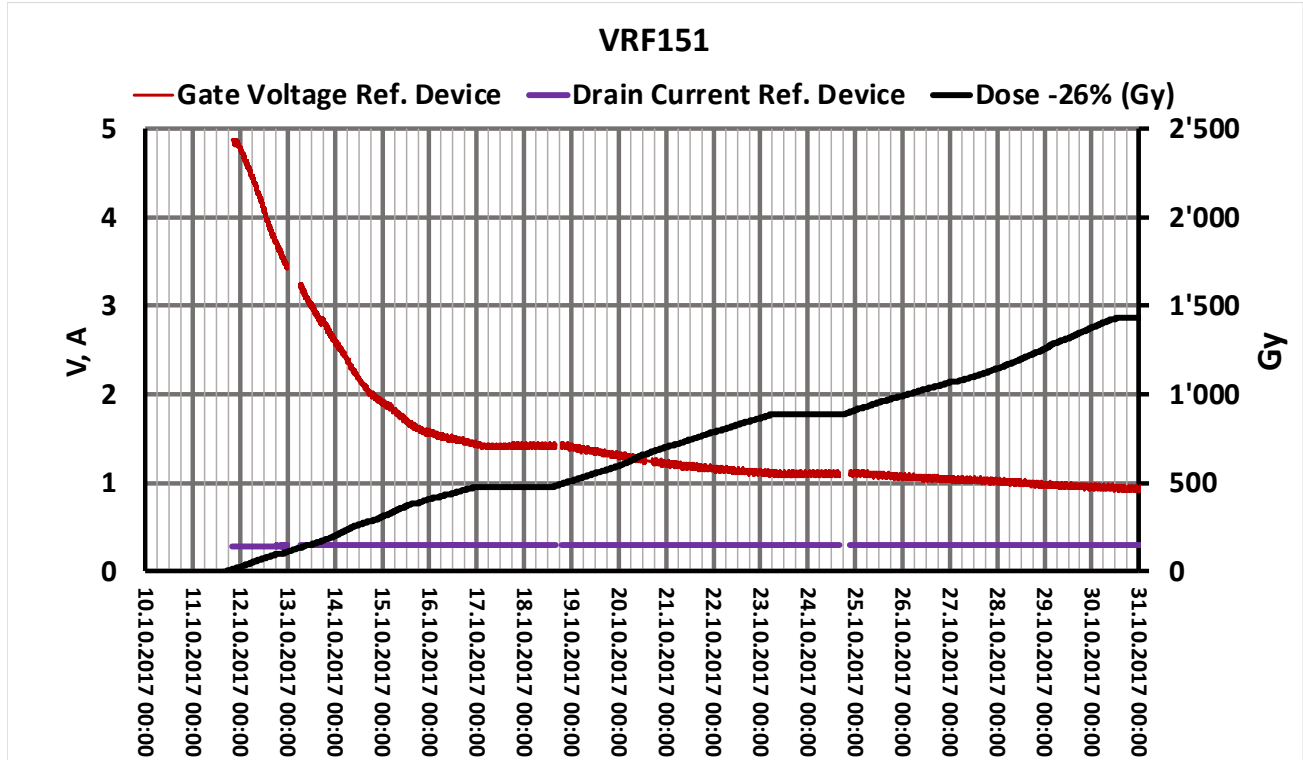


Figure 13: Reference Device Gate Voltage and Drain current and Dose received by VRF151.

The amplifier response proved quite stable showing a limited (≈ 1 dB) gain reduction at full dose and almost no phase rotation change.

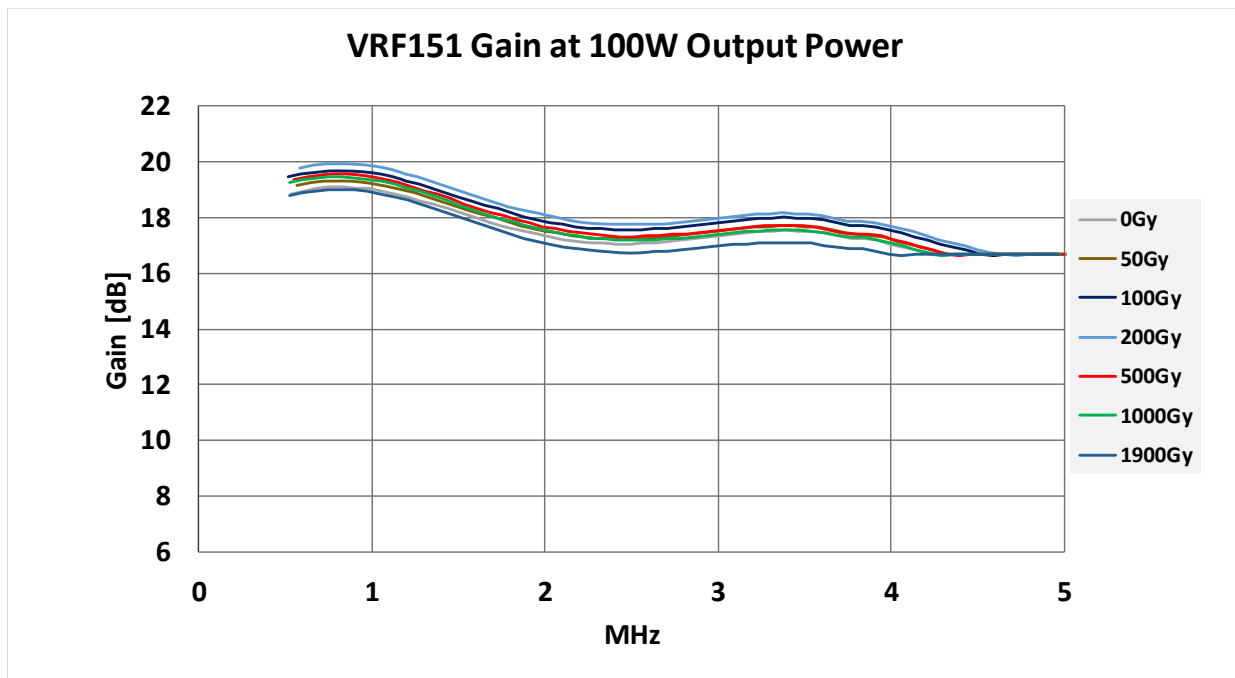


Figure 14: Gain response vs frequency at different TID.

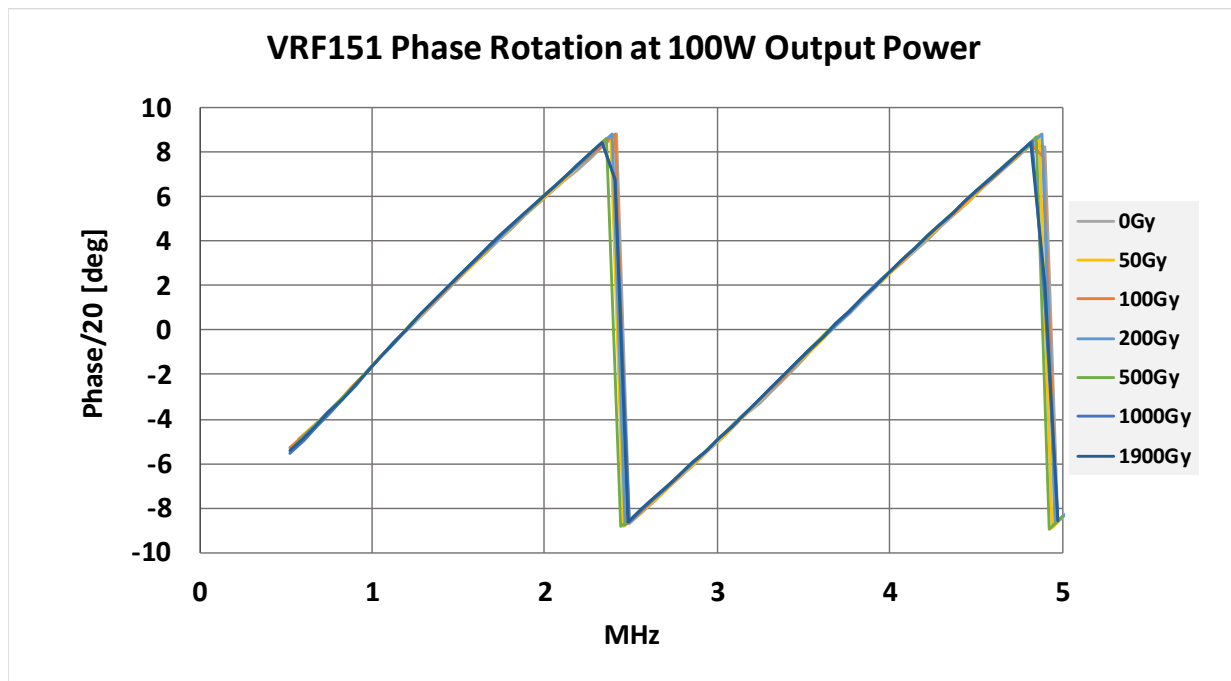


Figure 15: Phase rotation vs frequency at different TID.

9. Conclusions

Two RF power amplifiers, using VRF151 and BLF574 RF power mosfets were tested in CHARM facility to doses reaching 1.5-2kGy. The two amplifiers were operated sweeping the frequency range 0.5-5MHz and continuously producing 100W output power (as far as the devices could do it). The gate voltage was continuously controlled so as to compensate the V_{TH} displacement due to irradiation.

The system using the BLF574 device experienced an early failure in the control parts. The failure was independent from radiation. Despite the units could be operated until the end of the testing period and worked at satisfactory levels up 650Gy, the data collected are ambiguous and contradict data available in literature and previous measurements. Additional testing must be foreseen to draw final conclusions.

The system using the VRF151 device proved very good response. The V_{TH} displacement automatic compensation entirely fulfilled its function. Full power could be produced all along the testing period with limited gain changes and negligible phase shift variations.

No SE occurred.

[1] Charm UDD EDMS 1870824.

[2] "CHARM web site," [Online]. Available: <http://charm.web.cern.ch/CHARM/>.

[3] J. Mekki, M. Brugger, R. G. Alia, A. Thornton, . N. C. D. S. Mota and S. Danzeca, ""CHARM: A Mixed Field Facility at CERN for Radiation Tests in Ground, Atmospheric, Space and

Accelerator Representative Environments," *IEEE Trans. Nucl. Sci.*, vol. 63, no. 4, pp. 2016-2114, Aug 2016.

- [4] Spiezia G., P. Peronnard, A. Masi, M. Brugger, M. Brucoli, S. Danzeca, R. Garcia Alia, R. Losito, J. Mekki, P. Oser, R. Gaillard and L. Dusseau, "A New Radmon Version for the LHC and its Injection lines," *IEEE Trans. Nucl. Sci.*, vol. 61, no. 6, pp. 3424-3431, 2014.